ground water

Three-Dimensional Geostatistical Inversion of Flowmeter and Pumping Test Data

by Wei Li[1], Andreas Englert[2,3], Olaf A. Cirpka[4], and Harry Vereecken[2]

Abstract

We jointly invert field data of flowmeter and multiple pumping tests in fully screened wells to estimate hydraulic conductivity using a geostatistical method. We use the steady-state drawdowns of pumping tests and the discharge profiles of flowmeter tests as our data in the inference. The discharge profiles need not be converted to absolute hydraulic conductivities. Consequently, we do not need measurements of depth-averaged hydraulic conductivity at well locations. The flowmeter profiles contain information about relative vertical distributions of hydraulic conductivity, while drawdown measurements of pumping tests provide information about horizontal fluctuation of the depth-averaged hydraulic conductivity. We apply the method to data obtained at the Krauthausen test site of the Forschungszentrum Jülich, Germany. The resulting estimate of our joint three-dimensional (3D) geostatistical inversion shows an improved 3D structure in comparison to the inversion of pumping test data only.

Introduction

Pumping tests are one of the most common techniques to characterize the hydraulic properties of aquifers. In a pumping test, water is extracted or injected in a well and head changes are observed in adjacent wells. Conventional pumping tests using single pumping wells provide average properties of aquifers over a large influence zone, focusing on the regions between the pumping well and the monitoring wells. Combining multiple pumping tests in a tomographic format overcomes the drawback of single-well pumping by stressing and monitoring the aquifer at different locations (Neuman 1987; Butler and Liu 1993; Gottlieb and Dietrich 1995; Yeh and Liu 2000; Zhu and Yeh 2005, 2006; Bohling et al. 2007; Illman et al. 2007; Liu et al. 2007; Li et al. 2007). Since the various pumping tests show different patterns of sensitivity with respect to hydraulic parameters, they can provide a significantly improved description of aquifers. For pumping tests in fully screened wells, however, the system is stressed over the entire depth of the aquifer and only depth-averaged drawdown measurements are obtained. Thus, one can determine only depth-averaged properties of aquifers. However, sedimentary deposits often are heterogeneous in vertical direction since they typically contain lenses with large extension in horizontal directions but only limited thickness. Due to lacking vertical resolution, the estimates of hydraulic conductivity from pumping tests in fully screened wells are limited in the applicability to predict solute transport. Moreover, the effects of unresolved vertical variation of hydraulic conductivity on measured drawdown may be misinterpreted by assuming a too high apparent variance of storativity (Li et al. 2007). Such a high variance is conjectured to be biased because all the terms making up the storage coefficient hardly vary.

Borehole flowmeter tests (e.g., Molz et al. 1994; Zlotnik and Zurbuchen 2003) are a widely used approach to determine vertical profiles of hydraulic conductivities at well locations. In a flowmeter test, water is extracted from a fully screened well until it reaches steady state. Then, a flowmeter is used to continuously measure the vertical flow rates from the bottom of the well to the top of the screen. The increase of the flow rate over a certain

[1]Swiss Federal Institute of Aquatic Science and Technology (Eawag), Überlandstrasse 133, 8600 Dübendorf, Switzerland.
[2]Agrosphere, ICG-IV, Forschungszentrum Jülich GmbH, D-52425 Jülich, Germany.
[3]Currently at Lawrence Berkeley National Laboratory, Department of Earth Sciences, Cyclotron Road, Berkeley, CA 94720.
[4]Corresponding author: Swiss Federal Institute of Aquatic Science and Technology (Eawag), Überlandstrasse 133, 8600 Dübendorf, Switzerland; 41-44-8235455; fax: 41-44-823520; Olaf.Cirpka@eawag.ch
Received July 2007, accepted November 2007.

doi: 10.1111/j.1745-6584.2007.00419.x

depth increment relates to the hydraulic conductivity, K (m/s), at that location. From the measurements of flowmeter tests, one obtains only relative values of hydraulic conductivity. To obtain absolute values, the depth-averaged value of K at the well needs to be known (Javandel and Witherspoon 1969). To achieve these mean values, one has to rely on other tests, such as slug tests or small-scale pumping tests. In general, the depth averages vary with horizontal position so that an extra test for each well is needed. The conventional analysis of flowmeter tests becomes difficult for wells, for which unfortunately extra tests are not available. If a measurement of the depth-averaged hydraulic conductivity at a particular well is missing, one may try to estimate it from values obtained nearby, for example, from slug tests in different wells (e.g., Chen et al. 2001). These estimated average values are then used to convert the relative hydraulic conductivities to absolute values. Recently, Fienen et al. (2004) analyzed flowmeter tests using a geostatistical inverse method. Similar to conventional approaches, they need depth-averaged values of K at well locations. The depth-averaged values were considered as a known prior in the inference, which is an inconsistent requirement, because the mean value itself should be an outcome of the inversion. In some applications of geostatistical inversion, hydraulic conductivity values obtained by flowmeter tests are considered as direct measurements of local hydraulic conductivity (e.g., Rehfeldt et al. 1992; Chen et al. 2001). To the best of our knowledge, these measurements are considered as independent values in the cited studies. The K estimates derived from flowmeter tests, however, are correlated, which needs to be accounted for in conditioning.

In the present study, we jointly analyze data obtained by flowmeter and pumping tests in fully screened wells. We take the steady-state drawdowns of multiple pumping tests and the discharge profiles of flowmeter tests as our data. By directly using the discharge profiles, we do not require converting flowmeter test data to absolute hydraulic conductivities. In the joint analysis, the discharge profiles of flowmeter tests contain information about the vertical distribution of hydraulic conductivity, whereas values of steady-state drawdown obtained in fully screened wells during pumping tests contain information about horizontal fluctuations. In our approach, we fully consider how the measurements of flowmeter tests correlate, both in the computation of measurement errors and in the evaluation of sensitivities. We apply a full three-dimensional (3D) setup, also accounting for vertical flow in boreholes.

For the inversion, we follow the quasi-linear geostatistical approach of Kitanidis (1995) with extensions given by Nowak et al. (2003) and Nowak and Cirpka (2004). We apply the joint analysis to real measurements obtained at the Krauthausen test site in Germany (Vanderborght and Vereecken 2001; Vereecken et al. 1999, 2000).

Theory

Flowmeter Tests

To facilitate later descriptions, we briefly illustrate the setup of a flowmeter test in Figure 1. Here, b (m) refers to the aquifer saturated thickness, z_0 (m) stands for the reference level of the borehole bottom, and h (m) the height above the bottom. Extraction of water with a rate Q_p (m^3/s) is conducted until steady state is reached. Then, the vertical flow rate $Q(h)$ (m^3/s) within the borehole is measured by the flowmeter as a function of depth. The cumulative flow $Q(h)$ at height $z_0 + h$ can be expressed as follows:

$$Q(h) = \sum_i \Delta Q_i \tag{1}$$

in which ΔQ_i (m^3/s) is the induced flow at increment i within the total range of z_0 to $z_0 + h$. We assume that flow in the aquifer at the well radius is horizontal. Then, the relation between the horizontal hydraulic conductivity K_i (m/s) and the induced flow ΔQ_i (m^3/s) without ambient flow in a borehole can be quantified by (Javandel and Witherspoon 1969):

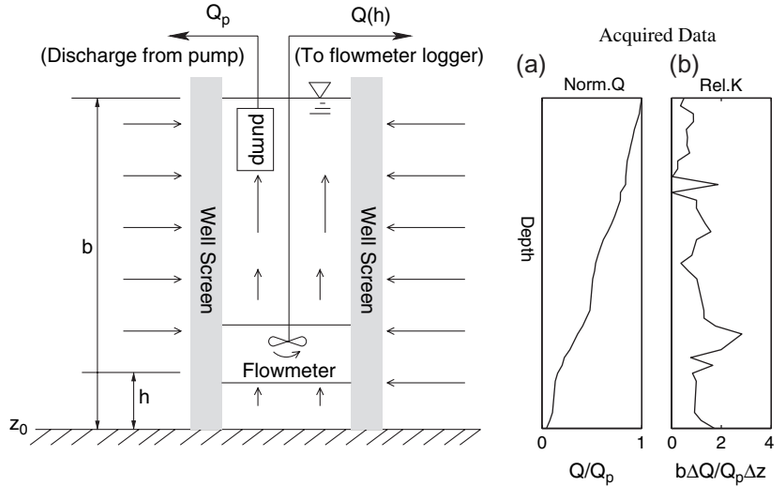

Figure 1. A typical setup of a flowmeter test and a graphic illustration of the data. (a) is the normalized cumulative discharge profile and (b) is the profile of relative hydraulic conductivities.

$$\eta_i = \frac{K_i}{\overline{K}} = \frac{\Delta Q_i b}{Q_\mathrm{p} \Delta z_i} \tag{2}$$

with

$$\overline{K} = \frac{\sum (K_i \Delta z_i)}{b} \tag{3}$$

where K_i is the hydraulic conductivity of the ith increment in the direct vicinity of the borehole, $\overline{K}$ (m/s) is the depth-averaged value of hydraulic conductivity over the depth of the borehole, and Δz_i (m) is the thickness of the ith measurement increment. We graphically illustrate the profiles of normalized discharges $Q(h)$ and the relative hydraulic conductivities in Figures 1a and 1b. In the following, the ratio η_i [-] of the measured discharge in the ith increment to the total discharge is denoted as discharge ratio.

The discharge ratio η_i does not explicitly depend on the depth-averaged value of hydraulic conductivity at the well location. Per flowmeter test, one vector $\boldsymbol{\eta}$ of discharge ratios is observed. Because $\boldsymbol{\eta}$ is a function of the differences of discharge rates between increments, the elements of $\boldsymbol{\eta}$ are correlated. We have to consider the correlation when defining the measurement error of $\boldsymbol{\eta}$.

For a particular flowmeter test, the sensitivity H_{ij} of the discharge ratio η_i with respect to the logarithm of hydraulic conductivity in cell j is zero everywhere except for the locations in the direct vicinity of the borehole where the test is conducted. We derive the corresponding H_{ij} based on Equations 2 and 3:

$$\begin{aligned} H_{ij} &= \frac{\partial \eta_i}{\partial \ln K_j} \\ &= \frac{\frac{\partial K_i}{\partial \ln K_j}\overline{K} - K_j \frac{\partial \overline{K}}{\partial \ln K_j}}{\overline{K}^2} \\ &= \frac{\frac{\partial K_i}{\partial \ln K_j}\overline{K} - K_i \frac{\partial \overline{K}}{\partial K_j}\frac{\partial K_j}{\partial \ln K_j}}{\overline{K}^2} \\ &= \frac{\delta_{ij} K_i \overline{K} - K_i \frac{\partial \overline{K}}{\partial K_j} K_j}{\overline{K}^2} \\ &= \delta_{ij}\eta_i - \eta_i \frac{\Delta Z_j}{b}\eta_j, \qquad i,j = 1 \ldots m_\eta \end{aligned} \tag{4}$$

in which δ_{ij}[-] is the Dirac delta function, which is 1 if $i = j$ and 0 otherwise. As shown, the sensitivity of $\boldsymbol{\eta}$ with respect to the logarithm of hydraulic conductivity is not a function of the absolute hydraulic conductivity at the well location. The discharge ratio at a certain depth, however, depends on the log-conductivity values along the entire depth of the well.

Using a Bayesian approach in the inversion, we need to quantify the uncertainty of the measurements due to measurement error. Considering that η_i, defined by the ratio of discharges, is not a direct measurement, we compute the measurement error $\sigma^2_{\eta_i}$ [-] of η_i through linear error propagation based on Equation 2:

$$\sigma^2_{\eta_i} = \frac{\sigma^2_{Q_i} + \sigma^2_{Q_{i-1}}}{Q^2_\mathrm{p}} \frac{b^2}{\Delta z_i^2} + \frac{\eta_i^2}{Q^2_\mathrm{p}} \sigma^2_{Q_\mathrm{p}} \tag{5}$$

in which $\sigma^2_{Q_i}$ (m^6/s^2) is the variance of the Q measurement at the ith increment, $\sigma^2_{Q_\mathrm{p}}$ (m^6/s^2) stands for the variance of the total discharge measurement. We assume that the measurement error between Q_i and Q_{i-1} is not correlated. The latter assumption may be put into question, for example, when the well is nonuniformly developed. While in principle, it is possible to include correlations between Q measurements in various depths, the information needed for that typically is not available. In any application, it is important that well construction and development are done carefully to minimize artifacts in the flowmeter measurements. It is advisory to analyze whether bypass flow, which may occur in high-permeability zones, affects the measurements (Dinwiddie et al. 1999). The quality of well construction may be tested by geophysical well-logging techniques. The cross covariance between the data of $\boldsymbol{\eta}$ is given by:

$$C_{\eta_i \eta_j} = \frac{\eta_i \eta_j}{Q^2_\mathrm{p}} \sigma^2_{Q_\mathrm{p}} - \left(\frac{\sigma^2_{Q_i}}{Q^2_\mathrm{p}} \delta_{j,i+1} + \frac{\sigma^2_{Q_{i-1}}}{Q^2_\mathrm{p}} \delta_{j,i-1} \right) \frac{b^2}{\Delta z_i^2} \tag{6}$$

Pumping Tests

We consider 3D flow in an aquifer that behaves like a confined one, that is, the drawdown is small in comparison to the water-saturated thickness. Prior to a particular pumping test, the system is assumed to be in steady state. After a sufficient time of pumping, the drawdown s (m) reaches steady state and can be described by the following equation:

$$-\nabla \cdot (K \nabla s) = W_0 \delta(\mathbf{x} - \mathbf{x}_\mathrm{w}) \tag{7}$$

with the boundary conditions:

$$s = 0 \quad \text{on } \Gamma_\mathrm{Diri} \tag{8}$$

$$\mathbf{n} \cdot \nabla s = 0 \quad \text{on } \Gamma_\mathrm{Neu} \tag{9}$$

in which K (m/s) is the hydraulic conductivity, W_0 (m^3/s) denotes the pumping rate (positive for extraction), $\delta(\mathbf{x} - \mathbf{x}_\mathrm{w})$ (1/m^3) is the Dirac delta function, $\mathbf{x}$ (m) is the vector of spatial coordinates, $\mathbf{x}_\mathrm{w}$ (m) is the location of the well, Γ_Diri and Γ_Neu denote Dirichlet and Neumann boundaries, and $\mathbf{n}$ [-] is the unit vector normal to the boundaries.

We calculate the sensitivity of drawdown with respect to log hydraulic conductivity Y using the continuous adjoint-state method (Sun and Yeh 1990):

$$\frac{\partial s}{\partial Y_i} = -\int_{Vi} \nabla \varphi \cdot \nabla s K \mathrm{d}x \tag{10}$$

in which V_i (m^3) is the volume related to a particular log-conductivity value Y_i, which is identical to a single element in our numerical implementation, and φ (m) is the adjoint state of drawdown described by:

$$-\nabla \cdot (K \nabla \varphi) = \delta(\mathbf{x} - \mathbf{x}_\mathrm{l}) \tag{11}$$

subject to the boundary conditions:

$$\varphi = 0 \text{ on } \Gamma_{\text{Diri}} \tag{12}$$

$$\mathbf{n} \cdot \nabla\varphi = 0 \text{ on } \Gamma_{\text{Neu}} \tag{13}$$

where $\delta(\mathbf{x} - \mathbf{x}_l)$ (1/s) is the Dirac delta function, and $\mathbf{x}_l$ is the location of measurements.

Inverse Kernel

Here, we briefly repeat the quasi-linear geostatistical approach to invert indirect measurements developed by Kitanidis (1995). We assume that the logarithm of hydraulic conductivity $Y(\mathbf{x})$ is a random spatial variable described by its mean and covariance function. We express $Y(\mathbf{x})$ by the sum of a deterministic trend and random fluctuations about the trend:

$$Y(\mathbf{x}) = \sum_{i=1}^{n_\beta} X_i(\mathbf{x})\beta_i + Y'(\mathbf{x}) \tag{14}$$

in which n_β is the number of deterministic base functions $X_i(\mathbf{x})$, β_i is a trend coefficient, and $Y'(\mathbf{x})$ is the spatially correlated random fluctuation about the deterministic trend. We consider that the joint pdf of $Y'(\mathbf{x})$ is (multi)-Gaussian, and thus fully described by the expected value of zero and the covariance function $R_{Y'Y'}(\mathbf{x})$ which is parameterized by a particular functional form, such as the exponential model, depending on a vector $\boldsymbol{\theta}$ of structural parameters, such as the variance and correlation lengths.

In numerical models, we discretize the spatial domain into n elements. The $n \times 1$ vector $\mathbf{Y}$ of discrete log hydraulic conductivity values are made of:

$$\mathbf{Y} = \mathbf{X}\boldsymbol{\beta} + \mathbf{Y}' \tag{15}$$

in which $\mathbf{X}$ is an $n \times n_\beta$ matrix of discretized base functions, $\boldsymbol{\beta}$ is an $n_\beta \times 1$ vector of trend coefficients, and $\mathbf{Y}'$ is the $n \times 1$ vector of the discrete fluctuations about the trend.

Our objective is to estimate the distribution of $\mathbf{Y}$ from an $n_m \times 1$ vector of measurements $\mathbf{Z}^m$, where n_m is the number of measurements. We achieve this by minimizing the following objective function:

$$\begin{aligned} L(\mathbf{Y}|\mathbf{Z}^m) = {} & \mathbf{Y}'^T\mathbf{R}_{\mathbf{Y}'\mathbf{Y}'}^{-1}\mathbf{Y}' + (\boldsymbol{\beta}-\boldsymbol{\beta}^*)^T\mathbf{R}_{\boldsymbol{\beta}\boldsymbol{\beta}}^{-1}(\boldsymbol{\beta} - \boldsymbol{\beta}^*) \\ & + (\mathbf{Z}^m - \mathbf{Z}(\mathbf{Y}))^T\mathbf{R}_{\mathbf{Z}\mathbf{Z}}^{-1}(\mathbf{Z}^m - \mathbf{Z}(\mathbf{Y})) \end{aligned} \tag{16}$$

in which $\mathbf{R}_{\mathbf{Y}'\mathbf{Y}'}$ is the $n \times n$ prior covariance matrix relating all log-conductivity values to each other, $\mathbf{Z}(\mathbf{Y})$ is the model outcome, and $\mathbf{R}_{\mathbf{Z}\mathbf{Z}}$ denotes the $n_m \times n_m$ covariance matrix expressing measurement error. Here, we assume that the difference between $\mathbf{Z}^m$ and $\mathbf{Z}(\mathbf{Y})$ using the correct log hydraulic conductivity values follows a multi-Gaussian distribution. We also consider that the trend coefficient $\boldsymbol{\beta}$ follows a multi-Gaussian distribution with the $n_\beta \times 1$ prior expected value $\boldsymbol{\beta}^*$ and the $n_\beta \times n_\beta$ prior covariance matrix $\mathbf{R}_{\boldsymbol{\beta}\boldsymbol{\beta}}$. $\boldsymbol{\beta}^*$ and $\mathbf{R}_{\boldsymbol{\beta}\boldsymbol{\beta}}$ must be estimated from existing information prior to interpreting the data. If no prior information exists, $\mathbf{R}_{\boldsymbol{\beta}\boldsymbol{\beta}}^{-1}$ becomes a zero matrix and $\boldsymbol{\beta}^*$ has no influence on the estimate. In Equation 16, the prior distributions of $\mathbf{Y}'$ and $\boldsymbol{\beta}$ are uncorrelated.

After some reformulation, it can be shown that the best estimate $\hat{\mathbf{Y}}$ of $\mathbf{Y}$ can be computed in an iterative manner by:

$$\hat{\mathbf{Y}}_{k+1} = \mathbf{X}\hat{\boldsymbol{\beta}}_k + \mathbf{R}_{\mathbf{Y}'\mathbf{Y}'}\mathbf{H}_k^T\hat{\boldsymbol{\xi}}_k \tag{17}$$

in which $\hat{\boldsymbol{\beta}}_k$ and $\hat{\boldsymbol{\xi}}_k$, are defined by:

$$\begin{aligned} & \begin{bmatrix} \mathbf{H}_k\mathbf{R}_{\mathbf{Y}'\mathbf{Y}'}\mathbf{H}_k^T + \mathbf{R}_{\mathbf{Z}\mathbf{Z}} & \mathbf{H}_k\mathbf{X} \\ \mathbf{X}^T\mathbf{H}_k^T & -\mathbf{R}_{\boldsymbol{\beta}\boldsymbol{\beta}}^{-1} \end{bmatrix} \begin{bmatrix} \hat{\boldsymbol{\xi}}_k \\ \hat{\boldsymbol{\beta}}_k \end{bmatrix} \\ & = \begin{bmatrix} \mathbf{Z}^m - \mathbf{Z}(\hat{\mathbf{Y}}_k) + \mathbf{H}_k\hat{\mathbf{Y}}_k \\ -\mathbf{R}_{\boldsymbol{\beta}\boldsymbol{\beta}}^{-1}\boldsymbol{\beta}^* \end{bmatrix} \end{aligned} \tag{18}$$

in which k is the iteration index and $\mathbf{H}_k$ is the $n_m \times n$ sensitivity matrix of the measurements with respect to the logarithms of hydraulic conductivity about the current estimate $\hat{\mathbf{Y}}_k$. In the present study, we consider $\boldsymbol{\theta}$ known, although methods are available to infer $\boldsymbol{\theta}$ from the measurements as well (Kitanidis 1995). We stabilize the inverse procedure with a modified Levenberg-Marquardt method (Nowak and Cirpka 2004), facilitating the application of spectral methods for the multiplication of sensitivities with the covariance matrix (Nowak et al. 2003).

For our joint analysis, $\mathbf{Z}^m$ is an aggregated vector:

$$\mathbf{Z}^m = [\mathbf{s} \quad \boldsymbol{\eta}] \tag{19}$$

in which $\mathbf{s}$ denotes the measurements of steady-state drawdown and $\boldsymbol{\eta}$ stands for the measurements of discharge ratios of flowmeter tests. In the inference, we compute the simulated drawdowns of our model and their adjoint-state variables using the finite-element method on a regular grid. Based on current hydraulic conductivity field, model outputs of the discharge ratios are simulated through Equations 2 and 3. The matrix of measurement error $\mathbf{R}_{\mathbf{Z}\mathbf{Z}}$ is made of:

$$\mathbf{R}_{\mathbf{Z}\mathbf{Z}} = \begin{bmatrix} \mathbf{R}_{\mathbf{Z}\mathbf{Z}}^{\mathbf{s}} & \mathbf{0} \\ \mathbf{0} & \mathbf{R}_{\mathbf{Z}\mathbf{Z}}^{\boldsymbol{\eta}} \end{bmatrix} \tag{20}$$

in which $\mathbf{R}_{\mathbf{Z}\mathbf{Z}}^{\mathbf{s}}$ is the matrix of measurement error of drawdowns and $\mathbf{R}_{\mathbf{Z}\mathbf{Z}}^{\boldsymbol{\eta}}$ of discharge ratios. We compute $\mathbf{R}_{\mathbf{Z}\mathbf{Z}}^{\boldsymbol{\eta}}$ using Equations 5 and 6. Here, matrix $\mathbf{H}$ is an aggregated matrix as well:

$$\mathbf{H} = \begin{bmatrix} \mathbf{H}^{\mathbf{s}} \\ \mathbf{H}^{\boldsymbol{\eta}} \end{bmatrix} \tag{21}$$

where $\mathbf{H}^{\mathbf{s}}$ is the sensitivity matrix of drawdown with respect to log hydraulic conductivity according to Equation 10 and $\mathbf{H}^{\boldsymbol{\eta}}$ is one of the discharge ratios, which is computed using Equation 4.

Site Description and Experimental Methods

Description of Test Site

The Krauthausen test site, operated by the Forschungszentrum Jülich, is located in the southern part of the Lower Rhine Embayment in Germany (Vanderborght and Vereecken 2001; Vereecken et al. 1999, 2000). It has an extension of 180 × 70 m. All

studies at the test site have focused on the uppermost aquifer with a thickness of approximately 10 m. The aquifer is part of a floodplain, consisting mainly of gravel and sand sediments. The site is equipped with 73 fully screened wells with approximately 5 cm diameter and a single well with approximately 17.5 cm diameter.

Analysis of borehole core materials demonstrates that the corresponding K values are well described by the lognormal distribution (Englert 2003). Vereecken et al. (2000) have shown that an exponential model for the covariance function can produce best fit with the data of core materials of the test site and the results of flowmeter tests discussed subsequently as well. From previous studies (Li et al. 2007) and preliminary investigation of the flowmeter data, we obtain the geostatistical structural parameters (Table 1) of log conductivity at the site. These parameters indicate that the field of hydraulic conductivity shows moderate heterogeneity with a strong horizontal to vertical anisotropy.

Field Campaign of Pumping and Flowmeter Tests

From March to August 2000, a series of small-scale pumping tests with a discharge rate of 2 m^3/h were conducted at 29 different pumping wells at the test site (Lamertz 2001). For each pumping test, approximately 10 wells adjacent to the production wells were used as observation wells. The distances of pumping and observation wells range from 1.63 to 130.91 m. Both the pumping and the observation wells were equipped with automatic loggers of hydraulic head with a resolution of 1 mm to measure and store the head changes at time intervals of 10 s. The pumping continued for 2 h. In Figure 2, we have plotted several drawdown curves. At later times, the measured data fluctuate about steady-state drawdown values. Well locations are marked by vertical gray solid lines and crosses in Figure 3.

In August 1994, flowmeter tests were conducted in 22 suitable wells (Schneider 1995). An electromagnetic borehole flowmeter was used in the tests. The vertical black solid lines and the circles in Figure 3 indicate the well locations. In the field, a pumping rate Q_p of 1.5 m^3/h was applied. A flowmeter was used to measure and record the flow rate Q_i in the wells as a function of depth. The vertical resolution of the measurements was 10 cm.

Table 1
Geometric and Geostatistical Parameters Used in the Inversion

Variable	Description	Value
Field domain and grid information		
L_1	Domain width (m)	70
L_2	Domain length (m)	200
L_3	Domain length (m)	8
Δx_1	Grid spacing in x_1 (m)	1
Δx_2	Grid spacing in x_2 (m)	1
Δx_3	Grid spacing in x_3 (m)	0.1
Geostatistical parameters		
σ^2	Prior variance of $\log_{10} K$ (K in m/s)	0.32
β^*	Prior mean of $\log_{10} K$ (K in m/s)	−2.8
$\sigma^2_{\beta^*}$	Uncertainty of prior mean β^*	0.19
λ_1	Correlation length in x_1 direction (m)	5.3
λ_2	Correlation length in x_2 direction (m)	5.3
λ_3	Correlation length in x_3 direction (m)	0.23

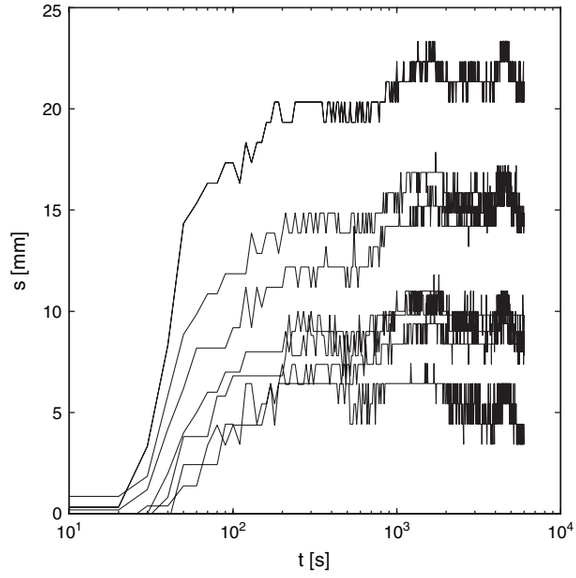

Figure 2. Example of drawdown curves in a single small-scale pumping test at Krauthausen, Germany. Here, seven monitoring wells are used.

Numerical Implementation

In our numerical implementation, we discretize the field on an orthogonal structured grid. State variables such as drawdown and its adjoint state are simulated using the finite-element method. The field dimensions and grid spacing used in the model are listed in Table 1.

In principle, one prefers to use grids allowing regional refinements around wells for pumping tests, rather than a regular grid. However, for unstructured grids, the efficient Fourier transformation methods for the evaluation of the covariance matrix will fail. For our application with 1.1 millions of unknowns, the evaluation of the covariance matrix on unstructured grids is computationally prohibitive. Although the application of Karhunen-Loève expansion to approximate the covariance function enables using an unstructured grid for large-scale problems of geostatistical inversion, previous two-dimensional studies have shown that the results on a regular grid are very close to the values on an unstructured one (Li and Cirpka 2006). Based on these considerations, we have applied a regular grid for our inverse model.

Since we use drawdown in our inversion, the influence of ambient flow is eliminated. In small-scale pumping test, we did not observe signals of drawdown on the horizontal edges of the field because the field dimension is much larger than the radius of influence of the small-scale pumping tests. Based on these observations, we have applied zero-drawdown boundary conditions on the boundaries forming vertical faces and no-flux boundary conditions on the top and the bottom of the aquifer.

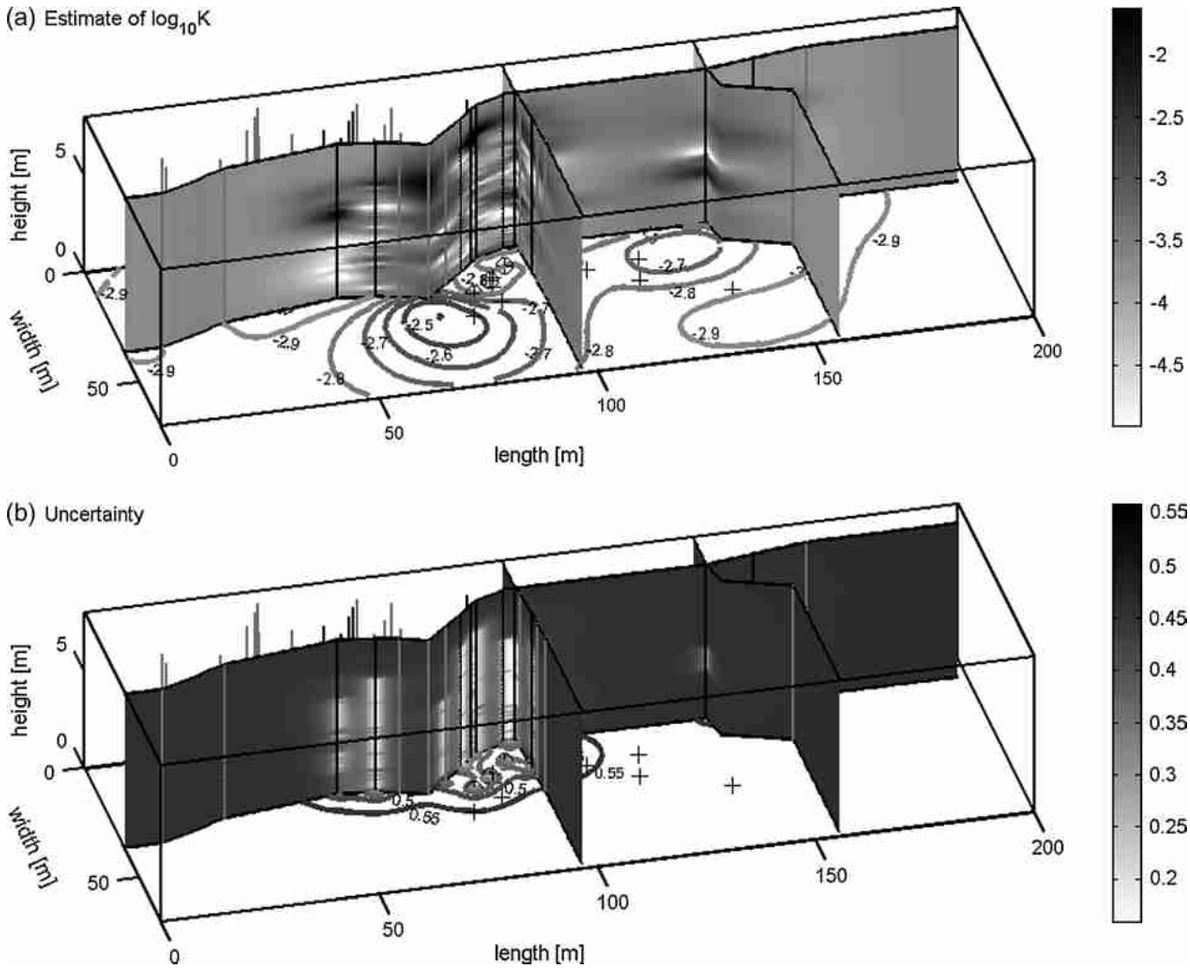

Figure 3. Results of joint geostatistical inversion of flowmeter and pumping test data. (a) is the estimate of $\log_{10} K$ with joint data of flowmeter and pumping tests and (b) displays the standard deviation of estimation of $\log_{10} K$ with joint data. Vertical black solid lines and the circles are the locations of the wells, where flowmeter tests were conducted; and the vertical gray lines and the crosses indicate the positions of the wells used in multiple pumping tests. Contour lines display the corresponding depth-averaged values.

The drawdown during the small-scale pumping tests was considerably smaller than the water-saturated thickness of the aquifer. Hence, it is permissible to analyze the steady-state pumping data assuming confined conditions.

In a flowmeter test, the sensitivity of incremental flux ΔQ_i with respect to log hydraulic conductivity is focused and decreases dramatically with increasing distance from the measurement location. The sensitivity approximately scales with $1/r^2$, where r is the distance to the measurement location. If near-well anomalies are not in the direct vicinity of the operating well, they hardly influence the flowmeter measurements. In our model, we have applied a resolution of 1 m in the horizontal directions. One single column of elements at the well location could capture most information of the flowmeter tests.

In our inverse procedure, we accounted for the small-scale pumping tests and flowmeter tests in a sequential way. We began with a single small-scale pumping test and all the flowmeter tests. Once optimal values of hydraulic conductivity were obtained, we added further pumping test data to the joint inversion, using the estimate from the previous step as initial guess for the following estimate. In each of these steps, all flowmeter data and an increasing number of pumping test data are jointly inverted. We repeatedly added pumping test data until all were used. In total, 175 measurements of drawdown and 808 observations of flowmeter data were considered.

The CPU time to estimate the approximated 1.1 million log-conductivity values was around 50 h on a 3GHz dual core PC operating under Linux.

Results

Figure 3 displays the resulting fields of log conductivity and its posterior uncertainty. Here, we select three vertical cross-section cutting through wells. Figure 3a shows log hydraulic conductivity after joint inversion of pumping test and flowmeter data. The contour lines on the bottom describe the distribution of depth-averaged values. Figure 3b shows the standard deviation of estimation. Again, the contour lines display the corresponding depth-averaged values. In Figure 3, the gray vertical lines

and the crosses indicate the locations of wells used for pumping tests and the black vertical lines and the circles are the well locations in flowmeter tests.

In Figure 3a, we clearly see that the 3D structure of hydraulic conductivity can only be revealed in the vicinity of wells where flowmeter tests were performed. In regions where only pumping test data exist, the estimated log-conductivity field becomes vertically uniform. Figure 3b shows that the remaining uncertainty of the estimated log hydraulic conductivity field decreases considerably near the wells used for flowmeter tests. That is, by adding flowmeter data to the inversion of pumping tests, the remaining uncertainty of hydraulic conductivity is reduced while vertical resolution is gained. We examine the variability of the obtained hydraulic conductivity near the wells used in flowmeter tests. For this purpose, we compute the variance of $\log_{10} K$ for all elements that are less than one correlation length away from such wells. The resulting variance is 0.06, which is considerably higher than 0.03, the variance of the entire estimated field. This confirms that resolution in the inversion is gained by adding flowmeter data to the pumping test data.

In Figure 4, we plot the fields of depth-averaged log conductivities inferred from joint inversion of flowmeter and pumping test data in comparison to the estimate derived from drawdown only. The patterns of depth-averaged log conductivity are almost identical in both cases. Figure 4c displays the difference of the two fields. The root mean square of the difference between the two fields is 0.086, indicating that the drawdown data provide a good estimate of the depth-averaged properties. For our test case, flowmeter data affect almost only vertical fluctuations of log conductivity in the inversion. These vertical fluctuations in turn hardly affect the simulated drawdown in the fully penetrated wells, so that, in our application, the depth-averaged conductivity could be inferred from pumping test data alone.

The validity of the estimate can be statistically tested by considering the orthonormal residuals (Kitanidis 1991). The sum of the squared orthonormal residuals should follow the χ^2 distribution with n_m degrees of freedom, where n_m is the number of measurements. For our test, the sum is 1056 which is within the 95% confidence interval for $n_m = 983$. Statistical validation, however, does not guarantee that the obtained estimate is sufficient

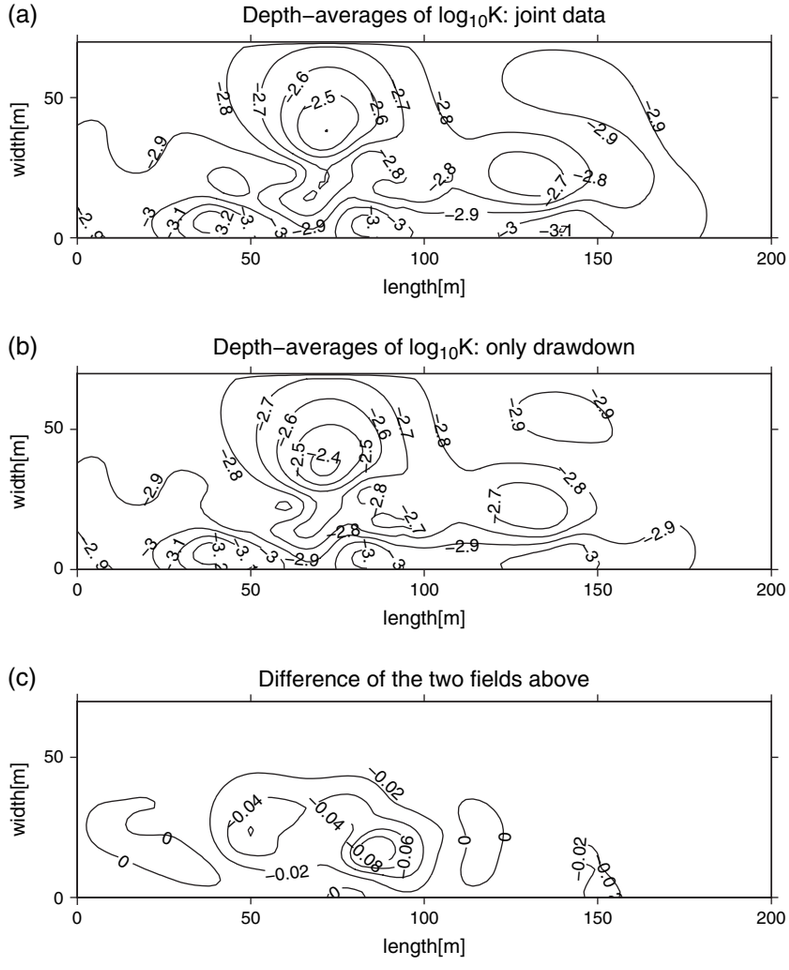

Figure 4. Fields of depth-averaged $\log_{10} K$ with joint data and with drawdown data only. (a) shows the depth-averaged values of $\log_{10} K$ with joint data, (b) shows depth-averaged $\log_{10} K$ with drawdown data only; and (c) shows the difference of the two depth-averaged fields.

for detailed predictive modeling. As is seen in Figure 3a, the 3D structure of the subsurface is revealed only in the direct vicinity of wells used in flowmeter tests. Eliminating a flowmeter test from our data base would result in an estimate lacking vertical resolution at the corresponding well. Because the associated estimation variance would also increase, measured flowmeter data at a well not included in the estimation would most likely remain within the predicted uncertainty bounds. That is, statistical cross validation is possible, but there are no redundant measurements. Any estimate with a reduced data set will result in deteriorated identification of subsurface structure. This makes validation beyond statistical tests difficult. At the field site, tracer tests have been performed. These data could be used for additional verification. A detailed analysis, whether the number of flowmeter tests performed at the site is already sufficient to predict the tracer test, however, is beyond the scope of the present study.

Discussion and Conclusions

We have obtained a 3D field of hydraulic conductivities by joint inversion of flowmeter and pumping test data applying the quasi-linear geostatistical inverse approach. The defined discharge ratios of flowmeter tests contain information about the vertical distribution of hydraulic conductivity at well locations; they need not be converted to absolute hydraulic conductivity values in the conditioning procedure. By jointly considering flowmeter and pumping test data, we overcome the disadvantage of providing only depth-averaged aquifer properties when pumping tests are performed using fully screened wells. The resulting estimate shows a significant improvement in identifying 3D structures. The inversion of pure drawdown data lacks vertical resolution but provides a good estimate of the depth-averaged hydraulic conductivity.

Inverting the discharge ratios alone would result in nonunique estimates. Since these ratios contain only relative information of hydraulic conductivity, the estimate based on these ratios is a relative value as well. Because the depth-averaged hydraulic conductivity may change with horizontal position, combining flowmeter data from several wells is difficult without additional data that are sensitive to the depth-averaged conductivity. Pumping test data are well suited for this purpose.

In this paper, we focused on the estimation of hydraulic conductivity. For this purpose, transient data of drawdown are not required; the conductivity field is inferred from the final steady-state drawdown alone. Transient head measurements would be required in the estimate of the storage coefficient. Although the flowmeter tests contain information only on hydraulic conductivities, the measured data have the potential to improve the estimate of storage coefficients because the transient drawdown depends on both hydraulic conductivity and storage coefficient. Any improvement in estimating hydraulic conductivity will reduce the chance of aliasing unresolved conductivity to storativity, thus leading to more reliable estimate of storage coefficient (Zhu and Yeh 2005; Li et al. 2007).

Flowmeter data are related to local hydraulic conductivity values. Thus, in the geostatistical framework, flowmeter measurements lead to modifications of the estimated conductivity field up to the distance of about one correlation length. This implies the necessity to place one fully screened well per correlation length if the 3D structure of hydraulic conductivity field is to be continuously resolved. A cost-efficient alternative would be to log relative hydraulic conductivity by direct-push techniques such as the direct-push permeameter (Butler et al. 2007). Structural information may also be gained by geophysical surveying although the relationship between properties inferred by geophysical assessments and hydraulic conductivity are not unique (e.g., Archie 1942; Purvance and Andricevic 2000; Salter and Lesmes 2002).

Acknowledgments

We thank associate editor Geoff Bohling, the two anonymous reviewers, and Walter Illman for their constructive suggestions.

References

Archie, G.E. 1942. The electrical resistivity log as an aid in determining some reservoir characteristics. Technical Report 1422. New York: American Institute of Mining, Metallurgical, and Petroleum Engineers.

Bohling, G.C., J.J. Butler, X. Zhan, and M.D. Knoll. 2007. A field assessment of the value of steady shape hydraulic tomography for characterization of aquifer heterogeneities. *Water Resources Research* 43, no. 5: W05430.

Butler, J.J., P. Dietrich, V. Wittig, and T. Christy. 2007. Characterizing hydraulic conductivity with the direct-push permeameter. *Ground Water* 45, no. 4: 409–419.

Butler, J.J., and W.Z. Liu. 1993. Pumping tests in nonuniform aquifers: The radially asymmetric case. *Water Resources Research* 29, no. 2: 259–270.

Chen, J.S., S. Hubbard, and Y. Rubin. 2001. Estimating the hydraulic conductivity at the South Oyster Site from geophysical tomographic data using Bayesian techniques based on the normal linear regression model. *Water Resources Research* 37, no. 6: 1603–1613.

Dinwiddie C.L., N.A. Foley, and F.J. Molz. 1999. In-well hydraulics of the electromagnetic borehole flowmeter. *Ground Water* 37, no. 2: 305–315.

Englert A. 2003. Measurement, estimation and modeling of ground water flow velocity at Krauthausen test site. Ph.D thesis, Fakultität für Bergbau, Hüttenwesen und Geowissenschaften, Rheinisch-Westfälischen Technischen Hochschule Aachen.

Fienen, M.N., P.K. Kitanidis, D. Watson, and P. Jardine. 2004. An application of Bayesian inverse methods to vertical deconvolution of hydraulic conductivity in a heterogeneous aquifer at Oak Ridge National Laboratory. *Mathematical Geology* 36, no. 1: 101–126.

Gottlieb, J., and P. Dietrich. 1995. Identification of the permeability distribution in soil by hydraulic tomography. *Inverse Problems* 11, no. 2: 353–360.

Illman, W.A., X. Liu, and A. Craig. 2007. Steady-state hydraulic tomography in a laboratory aquifer with deterministic heterogeneity: Multi-method and multiscale validation of hydraulic conductivity tomograms, *Journal of Hydrology* 341, no. 3–4: 222–234.

Javandel, I., and P.A. Witherspoon. 1969. A method of analyzing transient fluid flow in multilayered aquifer. *Water Resources Research* 5, no. 4: 856–869.

Kitanidis, P.K. 1991. Orthonormal residuals in geostatistics: Model criticism and parameter estimation. *Mathematical Geology* 23, no. 5: 741–758.

Kitanidis, P.K. 1995. Quasi-linear geostatistical theory for inversing. *Water Resources Research* 31, no. 10: 2411–2419.

Lamertz, F. 2001. Messung räumlicher Variabilität hydraulischer Parameter unter Anwendung von Pumpversuchen. Master's thesis. Lehrstuhl für Ingenieurgeologie und Hydrogeologie, Rheinisch-Westfälischen Technischen Hochschule Aachen.

Li, W., and O.A. Cirpka. 2006. Efficient geostatistical inverse methods for structured and unstructured grids. *Water Resources Research* 42, W06402, doi: 10.1029/2005WR004668.

Li, W., A. Englert, O.A. Cirpka, J. Vanderborght, and H. Vereecken. 2007. Two dimensional characterization of hydraulic heterogeneity by multiple pumping tests. *Water Resources Research* 43, no. 4: W04433.

Liu, X., W.A. Illman, A.J. Craig, J. Zhu and T.-C.J. Yeh. 2007. Laboratory sandbox validation of transient hydraulic tomography. *Water Resources Research* 43, no. 5: W05404, doi: 10.1029/2006WR005144.

Molz, F.J., G.K. Boman, S.C. Young, and W.R. Waldrop. 1994. Borehole flowmeters: Field application and data analysis. *Journal of Hydrology* 163, no. 4: 347–371.

Neuman, S.P. 1987. Stochastic continuum representation of fractured rock permeability as an alternative to the REV and fracture network concepts. In *Rock Mechanics: Proceedings of the 28th US Symposium*, ed. I.W. Farmer, J.J.K. Daemen, C.S. Desai, C.E. Glass, S.P. Neuman, and A.A. Balkema, 553–561. Rotterdam: the Netherlands.

Nowak, W., and O.A. Cirpka. 2004. A modified Levenberg-Marquardt algorithm for quasi-linear inversing. *Advances Water Resources* 27, no. 7: 735–750.

Nowak, W., S. Tenkleve, and O.A. Cirpka. 2003. Efficient computation of linearized cross-covariance and auto-covariance matrices of interdependent quantities. *Mathematical Geology* 35, no. 1: 53–66.

Purvance, D.T., and R. Andricevic. 2000. On the electrical-hydraulic conductivity correlation in aquifers. *Water Resources Research* 36, no. 10: 2905–2913.

Rehfeldt, K.R., J.M. Boggs, and L.W. Gelhar. 1992. Field study of dispersion in a heterogeneous aquifer: 3. Geostatistical analysis of hydraulic conductivity. *Water Resources Research* 28, no. 12: 3309–3324.

Salter, L., and D.P. Lesmes. 2002. Electrical-hydraulic relationships observed for unconsolidated sediments. *Water Resources Research* 38, no. 10: 1213.

Schneider, M. 1995. Charakterisierung der Variabilität der Permeabilität in einem quartären Grundwasserleiter. Master's thesis. Department of Engineering Geology and Hydrogeology, Rheinisch-Westfälischen Technischen Hochschule Aachen, and ICG-4, Forschungszentrum Jülich.

Sun, N.Z., and W.W.G. Yeh. 1990. Coupled inverse problems in ground water modeling. 1. Sensitivity analysis and parameter identification. *Water Resources Research* 26, no. 10: 2507–2525.

Vanderborght, J., and H. Vereecken. 2001. Analyses of locally measured bromide breakthrough curves from a natural gradient tracer experiment at Krauthausen. *Journal of Contaminant Hydrology* 48, no. 1–2: 23–43.

Vereecken, H., U. Döring, H. Hardelauf, U. Jaekel, U. Hashagen, O. Neuendorf, H. Schwarze, and R. Seidemann. 2000. Analysis of solute transport in heterogeneous aquifer: The Krauthausen field experiment. *Journal of Contaminant Hydrology* 45, no. 3–4: 329–358.

Vereecken, H., U. Döring, H. Hardelauf, U. Jaekel, O. Neuendorf, H. Schwarze, and R. Seidemann. 1999. Analysis of reactive solute transport in a heterogeneous aquifer. 1. Experimental set-up, sediment characterization and moment analyses. Interner Bericht 500699, Forschungszentrum Jülich.

Yeh, T.-C.J., and S. Liu. 2000. Hydraulic tomography: Development of a new aquifer test method. *Water Resources Research* 36, no. 8: 2095–2105.

Zhu, J., and T.-C.J. Yeh. 2005. Characterization of aquifer heterogeneity using transient hydraulic tomography. *Water Resources Research* 41, no. 7: W07028, doi: 10.1029/2004WR003790.

Zhu, J., and T.-C.J. Yeh. 2006. Analysis of hydraulic tomography using temporal moments of drawdown recovery data. *Water Resources Research* 42, no. 2: W02403, doi: 10.1029/2005WR004309.

Zlotnik, V.A., and B.R. Zurbuchen. 2003. Estimation of hydraulic conductivity from borehole flowmeter tests considering head losses. *Journal of Hydrology* 281, no. 1–2: 115–128.